frontiers in Materials

ORIGINAL RESEARCH
published: 16 August 2019
doi: 10.3389/fmats.2019.00189

Pressure Sensibility of Conductive Rubber Based on NBR- and Polypyrrole-Designed Materials

*Débora França[1], Ana Cláudia Rebessi[1], Fernanda Ferraz Camilo[2], Fernando G. Souza Jr.[3] and Roselena Faez[1]**

[1] Laboratório de Materiais Poliméricos e Biossorventes, Universidade Federal de São Carlos, Araras, Brazil, [2] Laboratório de Materiais Híbridos, Universidade Federal de São Paulo, Diadema, Brazil, [3] Instituto de Macromoléculas Professora Eloisa Mano, Universidade Federal do Rio de Janeiro, Rio de Janeiro, Brazil

Conductive rubbers combine features such as elasticity and electrical conductivities. Here, we developed an elastic conductive material based on nitrile rubber (NBR) and polypyrrole (PPy) by melt processing. PPy was also synthesized in three different media as silver (PPy-Ag), organomontmorillonite (PPy-OMt), and silver-organomontmorillonite (PPy-Ag-OMt) before mixture with NBR. Chemical structure, morphology, and stress–strain properties were evaluated. Pressure sensibility was evaluated in the range of 0–67 MPa during 10 cycles. During the compression and expansion processes, the electrical conductivity changes from high to low values and the difference of loading and unloading cycles demonstrates the repeatability and low hysteresis. The organomontmorillonite clay improves the homogeneity of particles into the matrix, and based on SEM images, the dispersity follows the sequence PPy-OMt, PPy-Ag-OMt, and PPy-Ag-OMt. This behavior affects the electrical conductivity and mechanical and electromechanical properties. The higher elastic modulus for composites compared to neat NBR is assigned to the reinforcing effect of the fillers. NBR/PPy-Ag-OMt (5 wt.%) is the best material in the absolute value of Scomp (46.3%/MPa) and the Scomp/hysteresis ratio (8.5%). In spite of different formulations displaying the best performance on the evaluated criteria (highest absolute conductivity, the highest percentage change in conductivity, lowest hysteresis, and lack of sample disruption), we can suggest that a lower amount of conducting particles benefits the reticulation process (as observed by the gel fraction values). Additionally, the possibility of using mechanical processing to obtain large-scale pressure sensor materials is without a doubt the most important outcome of this research area.

Keywords: conducting polymer, conductive rubber, melt processing, montmorillonite, silver

OPEN ACCESS

Edited by:
Guilherme Mariz de Oliveira Barra, Federal University of Santa Catarina, Brazil

Reviewed by:
Rafael Guntzel Arenhart, Federal University of Santa Catarina, Brazil
Marcos Akira D'Avila, Campinas State University, Brazil
Chayan Das, Visvesvaraya National Institute of Technology, India

***Correspondence:**
Roselena Faez
faez@ufscar.br

Specialty section:
This article was submitted to Polymeric and Composite Materials, a section of the journal Frontiers in Materials

Received: *19 March 2019*
Accepted: *24 July 2019*
Published: *16 August 2019*

Citation:
França D, Rebessi AC, Camilo FF, Souza FG Jr and Faez R (2019) Pressure Sensibility of Conductive Rubber Based on NBR- and Polypyrrole-Designed Materials. Front. Mater. 6:189. doi: 10.3389/fmats.2019.00189

INTRODUCTION

Pressure sensors are quite interesting materials to be used in areas such as medical and computer science (Job et al., 2003; Rosa et al., 2019). Conductive rubber is a composite material of an elastomeric matrix and conductive particles as a dispersed phase. Typically, the conductive particles are carbon composites and/or intrinsically conducting polymers (ICP) (Ali and Abo-Hashem, 1997; Cho et al., 1998; Sombatsompop et al., 2000; Das et al., 2002; Knite et al., 2004; Bing et al., 2010). This last class has attracted the attention of a wide academic and technological

field since they combine electrical properties, similar to metals, and mechanical properties and processability inherent to conventional polymers (Mattoso, 1996; Job et al., 2003; Swart et al., 2017; Sethi et al., 2018; Rosa et al., 2019). The addition of ICP in elastomers can combine the electrical and mechanical properties of these two classes of polymer in one (Hussain et al., 2001; Soto-Oviedo et al., 2006; Tran et al., 2018), allowing its application on technological fields such as pressure sensors, electric wires and cables coating, electrical contacts, carpet with antistatic properties, and others (Mravčáková et al., 2006; Bing et al., 2010). The electrical conductivity of conductive rubber depends on factors such as the nature of the elastomeric matrix and the type, size, structure, surface, and dispersion of the conductive particles as well as the test conditions, such as temperature and pressure (Ali and Abo-Hashem, 1997; Sombatsompop et al., 2000; Job et al., 2003; Bing et al., 2010). The conductor path is created by the different sizes and shapes of conducting particles homogeneously distributed and closer to each other (Hussain et al., 2001; Rosa et al., 2019). At the percolation threshold, the contact between the particles produces a conductive network that can be improved during the compression. From this phenomenon, the resistivity of the material reduces and its conductivity increases (Sombatsompop et al., 2000; Hussain et al., 2001; Job et al., 2003; Bing et al., 2010). However, elastomers–ICP composites still have challenges with the elastomeric cross-linking process (Prudêncio et al., 2014). Then, the use of an inorganic matrix [e.g., organomontmorillonite clay (OMt)] as a template for ICP synthesis is interesting to improve the compatibility of the conductive polymer and the elastomeric matrix, affording a material with superior mechanical properties (Baldissera and Ferreira, 2017). In addition, ICP produced in a confined environment, such as clays, produces a material with superior polymer chain organization and, consequently, higher electrical conductivity and thermal stability, which enables melt processing without degradation and/or electrical properties loss (Mravčáková et al., 2006; Soto-Oviedo et al., 2006; Rosa et al., 2019). Furthermore, the combination of silver nanoparticles with ICP improves the conductivity of the polymer (Wei et al., 2010) and opens the opportunity to use humidity and chemoreceptive sensors (Jlassi et al., 2013). The aim of this work was to prove the hypothesis that the insertion of fillers such as polypyrrole (PPy)-Ag, PPy-OMt, and PPy-Ag-OMt improves the processability and the conductive, thermal, and mechanical properties required for a pressure sensor.

EXPERIMENTAL

Chemicals

Pyrrole (Aldrich, P.A.), ammonium persulfate (APS; Aldrich, P.A.), cetyltrimethylammonium bromide (CTAB; Aldrich, P.A.), silver nitrate ($AgNO_3$; Aldrich, P.A.), sodium dodecyl sulfate (SDS; Aldrich, P.A.), sulfur (Aldrich, P.A.), stearic acid (Synth, P.A.), 2-mercaptobenzothiazole (MBTS-Fluka, PA), and zinc oxide (Synth, PA) were used as received. Bentonit Union (Brazilian trademark) provided montmorillonite clay. Organic-modified montmorillonite clay with ammonium quaternary salt (CTAB) in a weight ratio of salt:clay 1:1 (nominated OMt) was prepared as described in the literature (Fontana et al., 2013). Nitriflex SA, Brazil, provided nitrile rubber (NBR) with 30–34% acrylonitrile.

Preparation of PPy Composites (PPy-OMt; PPy-Ag; and PPy-Ag-OMt)

Polypyrrole (PPy) composites were prepared according to the previous work of França et al. (2017). Briefly, cationic (CTAB) and anionic (SDS) surfactants were dissolved in 100 ml of ultrapure water at a molar ratio of 1:5. Afterward, CTAB/SDS was added to the OMt dispersion (mass proportion of 1:1, PPy : OMt) and stirred for 2 h. Pyrrole (0.35 ml; 5.0 mmol) and APS (1.14 g; 5.0 mmol) were then added to the previous solution. The polymerization proceeded under magnetic stirring for 24 h. It was named PPy-OMt. For PPy-Ag-OMt composites, we used the same procedure, except for the silver nitrate ($AgNO_3$) (0.85 g; 5.0 mmol) used as an oxidant instead of the APS (França et al., 2017). For PPy-Ag, the same procedure for PPy-Ag-OMt was used except for the OMt absence. All samples were isolated by vacuum filtration using 0.22 μm hydrophilic PVDF membranes, washed several times with ultrapure water, and dried in a desiccator containing P_2O_5.

Preparation of NBR/PPy Composites

Conductive rubber containing PPy composites in a proportion of 5, 10, and 15 wt.% were mechanically mixed in a Haake Torque Rheometer mixer chamber with roller rotors. First, NBR was kept in the chamber for 2 min for mastication process, followed by the addition of the PPy composites at 150°C and 70 rpm for an additional 4 min, totaling 6 min of mixing. Secondly, at 100°C and 50 rpm, the vulcanizing agents were added in sequence: 5 wt.% of ZnO, 3 wt.% of stearic acid, 2 wt.% of sulfur, and 1 wt.% of MBT. Then, the material was passed under a roll mill and pressed under 6 tons in a hot press at 160°C for 10 min to complete the curing reaction.

Characterization

The fracture morphology images of the NBR/PPy composites containing 10 wt.% were taken in a field emission scanning electron microscope SEM-FEG JEOL (model JSM6701F) at 500× and 5,000× magnification using BS and SE detectors. Stress–strain behavior was performed according to DIN53504 Standard (DIN 53504, Germany, 1975) in a universal testing machine EMIC DL 2000 with a speed of 200 mm min^{-1}. The compression sensitivity test was conducted according to the method developed by Souza et al. (2005). The test was performed using a Keithley electrometer 6517A connected to the sample compartment and coupled to an Instron machine (Model 5569) using 10 cycles. The parameters of the experiment were as follows: a maximum force of 10,000 N, a test speed of 2 mm s^{-1}, and a maximum pressure of 62.70 MPa.

In order to better understand the cross-linking behavior of the elastomers, the soluble fraction (SF) and gel fraction (GF) were determined. Samples were soaked in methylethylketone (MEK) for 8 days. The difference between the swelled and dried samples was used to determine the SF and GF.

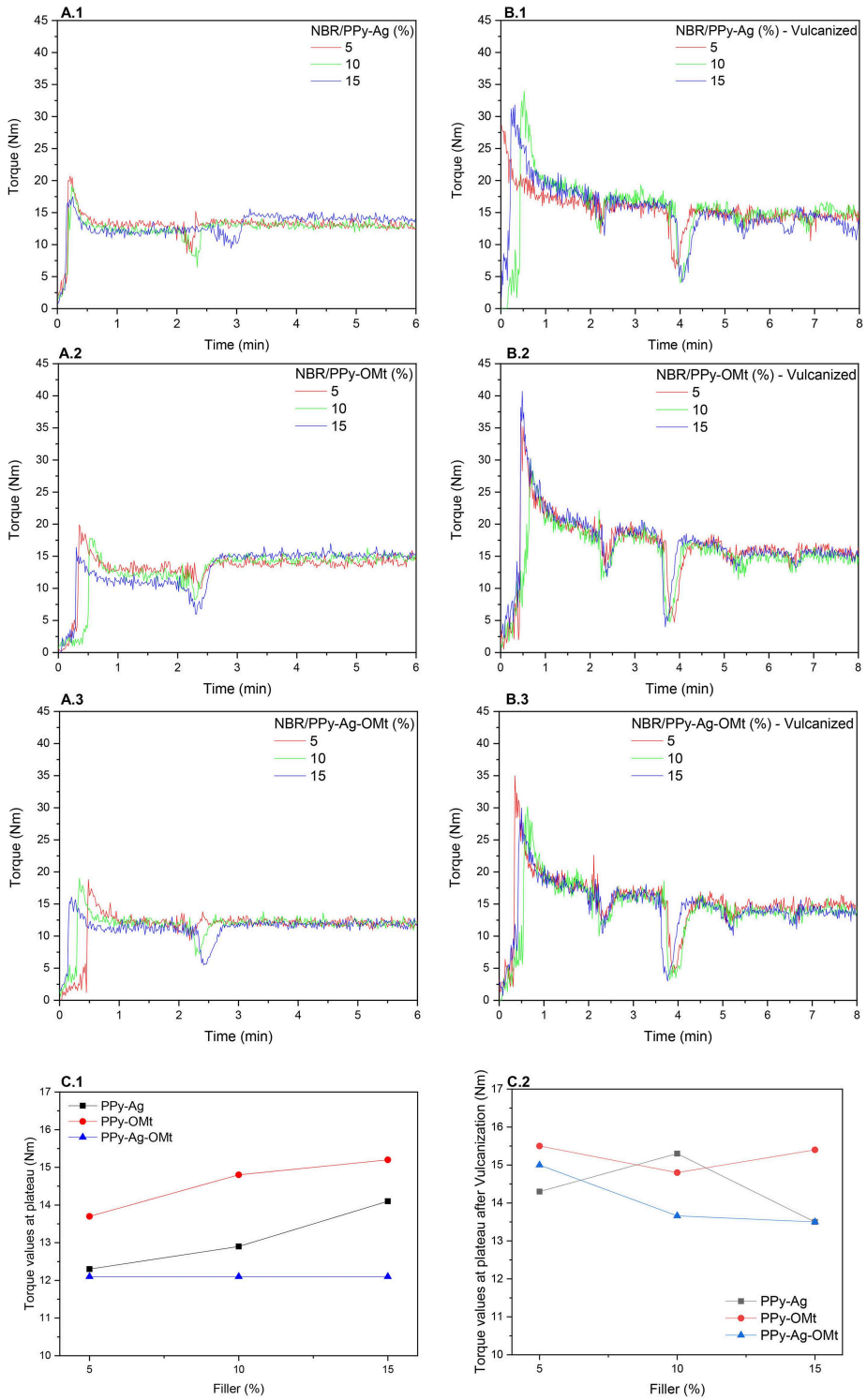

FIGURE 1 | Torque curves of NBR/PPy composites. **(A.1–A.3)** Components mixing curves; **(B.1–B.3)** NBR/PPy composites combined with the vulcanizing system; and **(C.1,C.2)** torque values at the plateau vs. PPy composite loadings.

RESULTS AND DISCUSSION

Figure 1 shows the torque curves of the NBR/PPy composite mixing (**Figure 1A**), NBR/PPy composites combined with the vulcanizing system (**Figure 1B**), and torque values at the plateau vs. PPy composite loadings (**Figure 1C**). From torque curves, we can follow the mixing behavior of the components of the mixture independent of the PPy composite types. At the beginning of

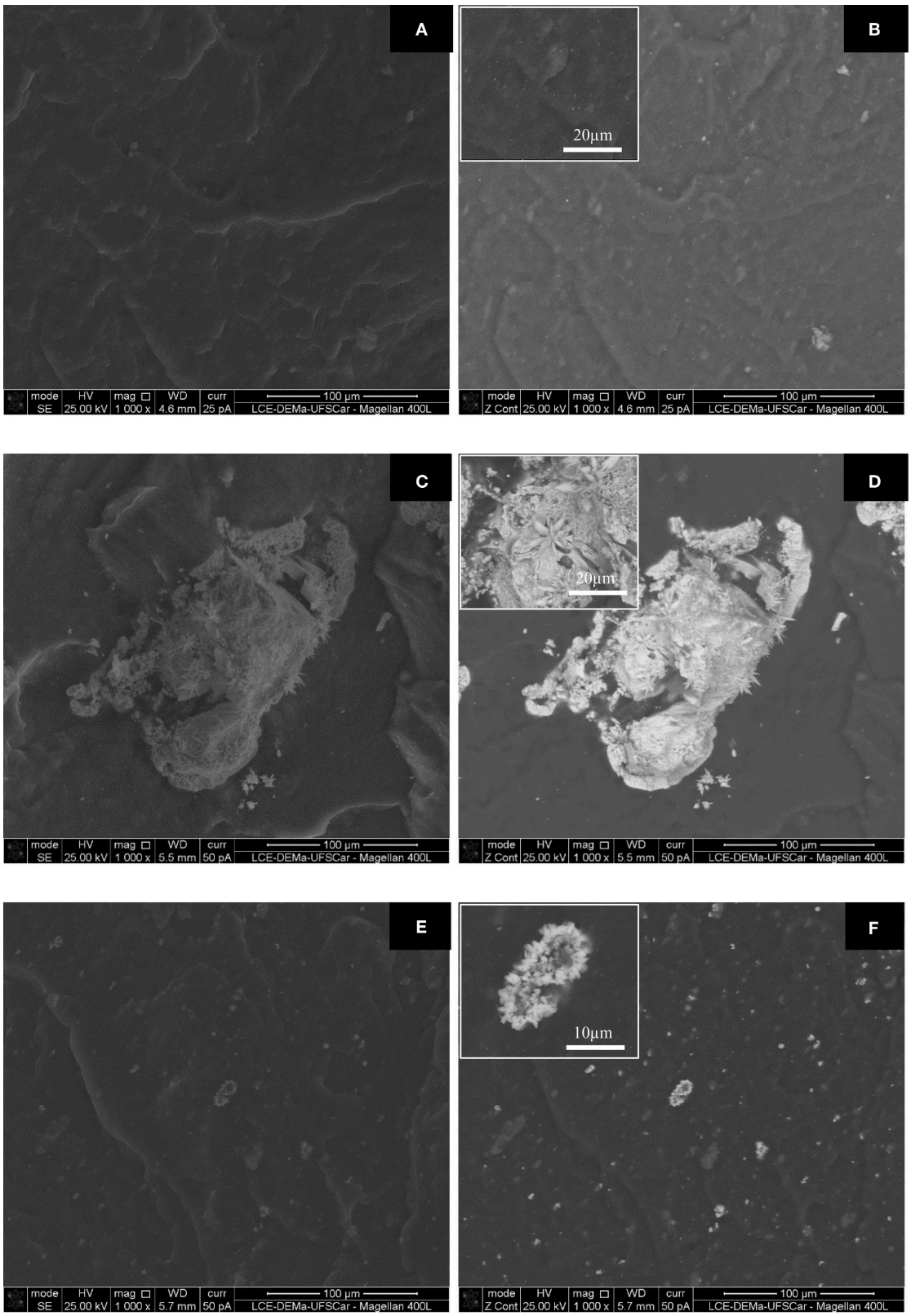

FIGURE 2 | SEM fracture morphology of NBR with 10 wt.% of **(A,B)** PPy-OMt, **(C,D)** PPy-Ag, and **(E,F)** PPy-Ag-OMt. **(A,C,E)** are images of secondary electrons and **(B,D,F)** are images of backscattered electrons.

the mixture, the increase of the torque (∼30 s) is assigned to the NBR addition in the chamber followed by a torque decrease due to the mastication process. After 2 min, a torque decrease shown as a peak is attributed to the chamber opening to add PPy composites, and the mixing process continued until reaching a plateau (6 min). The torque curves of the NBR/PPy composites during the insertion of the vulcanizing system (**Figure 1B**) shows four peaks at ∼30, 60, 150, 300, and 390 s assigned, respectively, to the addition of the ZnO, stearic acid, sulfur, and MBT. After the whole vulcanizing system was inserted, the process continued for 90 s to guarantee that no reticulation reaction started to occur inside the mixing chamber. The reticulation only occurred during the molding at 160°C in the hot press (6 tons for 10 min). **Figures 1C.1, C.2** compare the torque values at the plateau for the different PPy composites before and after vulcanization, respectively. The sequence of torque values, independently of the filler amount, is NBR/PPy-OMt > NBR/PPy-Ag > NBR/PPy-Ag-OMt. Higher torque values at the plateau represent a harder mixture and imply better interaction among the components, mainly the aggregation of the filler into the matrix. Also, we observe the influence of the amount of filler for PPy-OMt, which corroborated the hypothesis of better interaction of the filler with NBR (Thomas and Maria, 2017). PPy-Ag shows intermediate performance with a slight increase for superior filler loading; PPy-Ag-OMt displays no influence of the filler amount. Besides, no significant differences of the torque values at the plateau for composites after the addition of vulcanizing system were observed (**Figure 1C.2**).

Figure 2 shows the fracture morphology of the NBR/PPy-OMt, NBR/PPy-Ag, and NBR/PPy-Ag-OMt, all of them with 10 wt.% of PPy composite. A backscattered electron (BSE) detector (**Figures 2B,D,F**) was used in order to show the difference in contrast over the SEM images. Brighter BSE images are shown for material prepared with an element with a high atomic number. In this way, the dispersity of nanosilver particles can be identified as well as the inorganic material dispersed

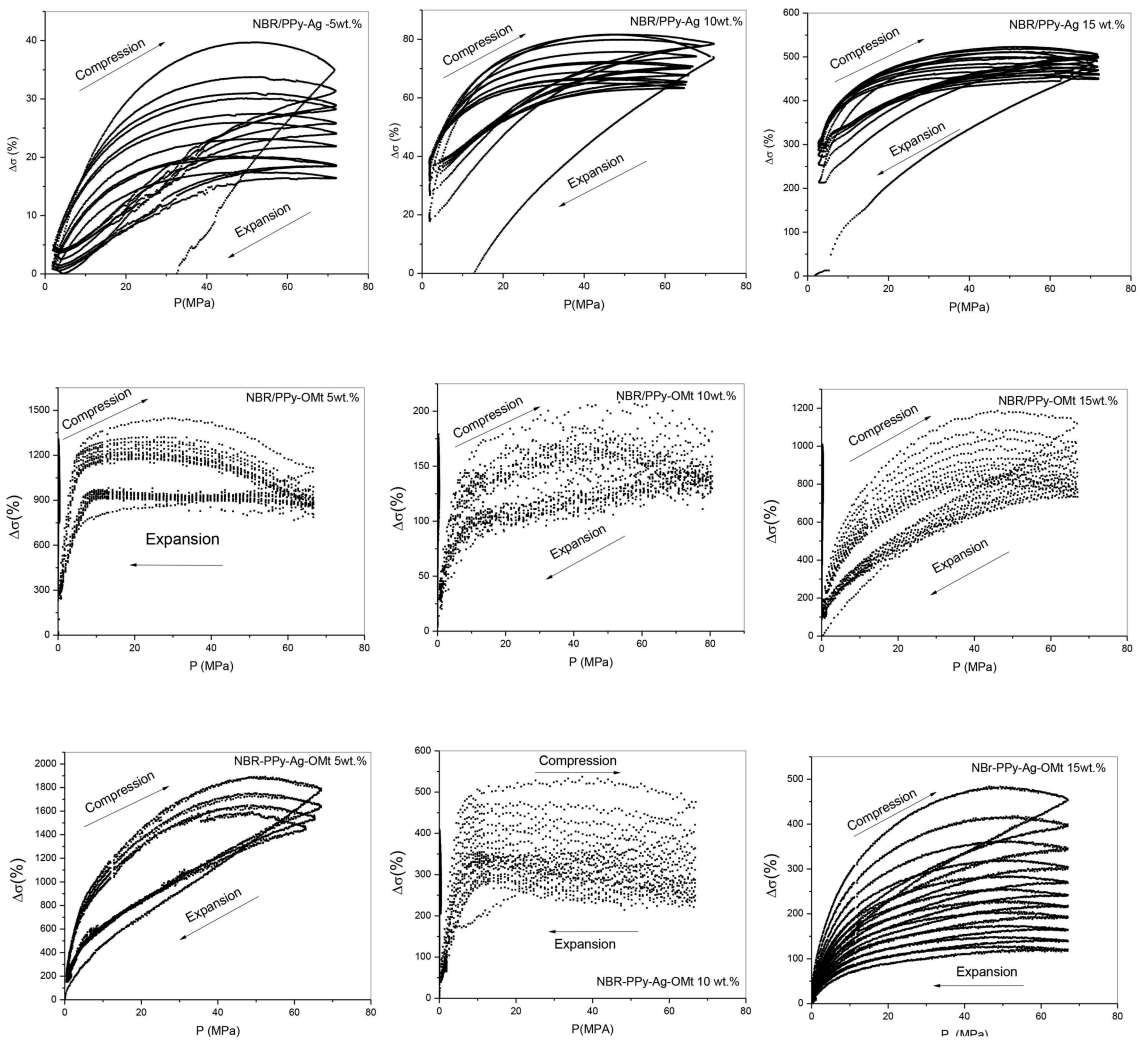

FIGURE 3 | Compression–expansion curves of NBR-PPy-Ag, NBR-PPy-OMt, and NBR-PPy-Ag-OMt.

TABLE 1 | Electrical conductivity, elastic modulus, maximum stress, maximum strain, and gel fraction of NBR/PPy-OMt, NBR/PPy-Ag, and NBR/PPy-Ag-OMt conductive rubbers.

Sample (wt.%)		Conductivity $\times 10^{-6}$ (S cm^{-1})	Elastic module [E(MPa)]	Tension at break [σ(MPa)]	Deformation at rupture [ε (%)]	GF (%)
NBR pure		—	1.8 ± 0.20	4.60 ± 0.40	443 ± 42	92
NBR/PPy-OMt	5	0.040 ± 0.022	2.50 ± 0.08	5.54 ± 0.73	412 ± 13	98
	10	0.50 ± 0.32	2.82 ± 0.35	7.22 ± 1.06	430 ± 50	97
	15	6.60 ± 0.88	3.65 ± 0.53	9.39 ± 0.75	453 ± 50	96
NBR/PPy-Ag	5	10.00 ± 1.50	2.32 ± 0.19	5.35 ± 1.19	425 ± 63	92
	10	14.30 ± 1.60	1.81 ± 0.80	4.85 ± 0.67	457 ± 67	86
	15	33.00 ± 2.30	2.38 ± 0.62	3.52 ± 1.42	607 ± 126	86
NBR/PPy-Ag-OMt	5	1.30 ± 0.65	1.83 ± 0.16	5.04 ± 0.52	431 ± 56	97
	10	7.70 ± 2.80	2.47 ± 0.25	4.86 ± 0.77	450 ± 55	95
	15	12.50 ± 2.60	1.51 ± 0.43	6.03 ± 0.44	791 ± 175	89

TABLE 2 | Electromechanical properties.

Sample-wt.%	Δσ (%) @ Pmax/2 (%)	S_{Comp} (%/Mpa) @ Pmax/2	Hysteresis (%) @ Pmax/2
NBR/PPyAg-5	20.0 ± 2.9	0.6 ± 0.1	13.0 ± 2.7
NBR/PPyAg-10	71.9 ± 5.8	2.1 ± 0.2	8.9 ± 6.6
NBR/PPyAg-15	484.8 ± 20.5	13.9 ± 0.6	45.9 ± 9.8
NBR/PPyOMt-5	1,252.6 ± 81.9	35.8 ± 2.3	342.1 ± 68.3
NBR/PPyOMt-10	173.7 ± 14.5	5.0 ± 0.4	60.9 ± 6.4
NBR/PPyOMt-15	983.5 ± 96.9	28.1 ± 2.8	254.3 ± 53.2
NBR/PPyAgOMt-5	1,621.8 ± 91.7	46.3 ± 2.6	559.6 ± 56.1
NBR/PPyAgOMt-10	419.9 ± 55.8	12.0 ± 1.6	155.4 ± 33.0
NBR/PPyAgOMt-15	321.0 ± 72.5	9.2 ± 2.1	170.6 ± 33.2

on the elastomeric matrix. Inserted images at **Figures 2B,D,F** are at high magnifications to show the morphology of the particles into de NBR. Conductive rubbers with 5 and 15 wt.% of PPy composite displayed similar morphology and are not shown here. We observe a high dispersity and homogeneity of PPy-OMt particles into an NBR with a smooth surface. The morphology reflected the torque results since the homogeneous morphology aspect is related to a good interparticle interaction among components (**Figures 2A,B**). The morphologies of NBR/PPy-Ag and NBR/PPy-Ag-OMt (**Figures 2C–F**, respectively) were analyzed as a function of the presence of Ag nanoparticles and OMt. We also observe higher homogeneity but small clusters dispersed in the matrix. According to the BSE images (**Figures 2D,F**) we assigned the white images to the Ag in which the particles are clumped in the pointed stars shape. This morphology is quite interesting since the agglomerations improve the performance of the material during the compression-expanded cycles due to the particle–particle contact (**Figure 3**; Souza et al., 2005; Thomas and Maria, 2017). It is interesting to note the decrease of the particle size and also the improvement of the dispersion and homogeneity of the particle into the NBR rubber matrix comparing PPy-Ag and PPy-Ag-OMt composites.

Table 1 shows the electrical conductivity and mechanical properties of the NBR composites. The electrical conductivity values are in the order of 10^{-6} to 10^{-8} S cm^{-1}, which characterizes semiconducting material. The sequence of the conductivity of the material is due to the presence of the nanosilver, i.e., NBR/PPy-OMt < NBR/PPy-Ag-OMt < NBR/PPy-Ag. This behavior is in accordance with the value of neat particle conductivity (França et al., 2017) and the contact between the dispersed particles in the NBR matrix. Mechanical properties depicted as elastic modulus, tension, and deformation at break show discrepant values according to the amount and type of the conducting particles. Elastic modulus represents the rigidity or stiffness of a material. Compared to the neat NBR, we observed higher elastic modulus for composites, corroborating the reinforcing effect of the filler on the elastomeric matrix. NBR/PPy-OMt show higher values and increase with the filler content. However, in NBR/PPy-Ag and NBR/PPy-Ag-OMt, besides the lower values, no linearity is observed according to the filler amount. This behavior is assigned to the GF values. GF measures the degree of the reticulation of the material, and lower values are due to the solubilization of the elastomer not cross-linked. Since the reticulation is lower, the module also decreases. The tensile strength at break is higher for PPy-OMt, but Ag particles decrease the strength. This behavior can be assigned to the agglomeration of the particles that generate points of fragility in the material. Both properties, module and strength, corroborate with the largest deformation of PPy-Ag and PPy-Ag-OMt composites.

Figure 3 shows the expansion–compression cycles and **Table 2** shows the electromechanical properties of NBR/PPy-Ag, NBR/PPy-OMt, and NBR/PPy-Ag-OMt. In order to correlate the data sets supplied by the Instron machine and the electrometer, a method was followed as summarized: The percentage variation of the sample conductivity ($\Delta\sigma$) is calculated in accordance with Equation (1).

$$\Delta\sigma = \frac{100x(R^{-1} - R_0^{-1})}{R_0^{-1}} \quad (1)$$

Experimental data obtained during compression (loading) and expansion (unloading) are treated separately. The average hysteresis ($\bar{h}$) is calculated in accordance with Equation (2).

$$\overline{h} = \sum_{j=1}^{n} \frac{(\Delta\sigma_{c(j)} - \Delta\sigma_{d(j)})}{n} \quad (2)$$

where n is the number of compression and expansion cycles and $\Delta\sigma_{c(j)}$ and $\Delta\sigma_{d(j)}$ represent the percentage variation of the sample conductivity obtained during the jth compression and expansion cycles, respectively. $\Delta\sigma_{c(j)}$ and $\Delta\sigma_{d(j)}$ are taken at the half of the maximum applied pressure. The compression sensitivity (*Scomp*) can be defined as shown in Equation (3).

$$\text{Scomp} = \left(\frac{\Delta\sigma}{\Delta P}\right) \quad (3)$$

and can be computed for each data pair ($\Delta\sigma$ vs. P) during compression and expansion cycles. Finally, the average *Scomp* can be calculated as shown in Equation (4).

$$\overline{\text{Scomp}} = \sum_{j=1}^{n} \frac{\left(\Delta\sigma_{(j)} P_{(j)}\right)}{n} \quad (4)$$

For NBR/PPy-Ag materials, as PPy-Ag content is increased, the higher is the compression sensitivity. By increasing content, the contact between the particles is improved, and as these particles are large in size and the dispersity is lower (as observed in SEM images), a higher concentration is necessary to have contact and, consequently, conductivity. The linearity was not observed for NBR/PPy-OMt and NBR/PPy-Ag-OMt. Both material composites with 5 wt.% PPy-OMt or PPy-Ag-OMt showed higher Scomp (35.8 and 46.3%/MPa, respectively), besides higher hysteresis. However, comparing the relative percentage of Scomp/hysteresis values of 10.5% and 8.5%, it is found that NBR/PPy-Ag-OMt (5 wt.%) is the best material in terms of absolute value of Scomp and Scomp/hysteresis ratio. In spite of the different formulations displayed and the best performance on the evaluated criteria (highest absolute conductivity, the highest percentage change in conductivity, lowest hysteresis, and lack of sample disruption), we can suggest that a lower amount of conducting particles benefits the reticulation process (as observed by the GF values). Also, considering the 16 vol.% general concentration of particles to achieve the percolation threshold, the materials we prepared are below this value and can contribute to particle contact during expansion–compression cycles (Schueler et al., 1997). Besides, the clay improved the dispersion of the particles in the NBR, which helps to decrease the necessary amount of filler to the performance of the material. The properties of the conductive rubbers can be influenced by the amount of filler used, in the way it interacts with the matrix and with the other filler particles. Song (2017) compared micro- and nanofillers used as reinforcement and emphasized how organic modifications, coupling agents, and better dispersion control techniques influence the interaction between the rubber matrix and the fillers as we observed in our work.

CONCLUSION

Conductive rubber based on NBR added with PPy composites has shown interesting properties to be applied in the pressure sensor. Among the samples, NBR/PPy-Ag 15 wt.% was highlighted because of the highest volume conductivity and lower hysteresis attained. On the other hand, the NBR/PPy-Ag-OMt 5% proved to be the best material in terms of absolute value of Scomp and the Scomp/hysteresis ratio. These results were related to morphological aspects, where the particles are shown to be dispersed, and the amount and the type of filler played an important role to the connected–disconnected system between particles that could happen during the compression–expansion cycles.

DATA AVAILABILITY

All datasets generated for this study are included in the manuscript and/or the supplementary files.

AUTHOR CONTRIBUTIONS

DF and AR performed the materials preparation and the structural, morphological, stress-strain, and conductivities measurements. RF was involved in planning and supervised the work. FC was involved in planning and PPy-Ag synthesis. FS performed the pressure sensibility measurements. RF and FS interpreted the pressure sensibility results. DF and RF processed the experimental data, performed the analysis, drafted the manuscript, and designed the figures. All authors discussed the results and commented on the manuscript.

ACKNOWLEDGMENTS

Thanks to FAPESP (07/50742-2, 08/57706-4, and 11/23742-7) for financial support. RF and FC are CNPq researchers.

REFERENCES

Ali, M. H., and Abo-Hashem, A. (1997). The percolation concept and the electrical conductivity of carbon black-polymer composites. 3. Crystalline chloroprene rubber mixed with FEF carbon black. *J. Mater. Process. Tech.* 68, 168–171. doi: 10.1016/S0924-0136(96)00023-4

Baldissera, A. F., and Ferreira, C. A. (2017). "Clay-based conducting polymer nanocomposites," in *Conducting Polymer Hybrids*, eds V. Kumar, S. Kalia, and H. C. Swart (Cham: Springer International Publishing), 143–163.

Bing, G., Lan, Q., and Biao, W. (2010). Study on pressure and temperature characteristics of sensitive rubber composite. *Adv. Mat. Res.* 143–144, 134–138. doi: 10.4028/www.scientific.net/amr.143-144.134

Cho, M. S., Choi, H. J., and To, K. (1998). Effect of ionic pendent groups on a polyaniline-based electrorheological fluid. *Macromol. Rapid Commun.* 19, 271–273. doi: 10.1002/marc.1998.030190601

Das, N. C., Chaki, T. K., and Khastgir, D. (2002). Effect of axial stretching on electrical resistivity of short carbon fibre and carbon black filled conductive rubber composites. *Polym. Int.* 51, 156–163. doi: 10.1002/pi.811

Fontana, J. P., Camilo, F. F., Bizeto, M. A., and Faez, R. (2013). Evaluation of the role of an ionic liquid as organophilization agent into montmorillonite for NBR rubber nanocomposite production. *Appl. Clay Sci.* 83–84, 203–209. doi: 10.1016/j.clay.2013.09.002

França, D., Rebessi, A. C., Rubinger, C. P. L., Ribeiro, G. M., Camilo, F. F., and Faez, R. (2017). Structural and conductivity relationship of binary and ternary composites of polypyrrole, montmorillonite and silver. *J. Nanosci. Nanotechnol.* 17, 9203–9210. doi: 10.1166/jnn.2017.14302

Hussain, M., Choa, Y.-H., and Niihara, K. (2001). Fabrication process and electrical behavior of novel pressure-sensitive composites. *Compos. Part A: Appl. Sci. Manuf.* 32, 1689–1696. doi: 10.1016/S1359-835X(01)00035-5

Jlassi, K., Singh, A., Aswal, D. K., Losno, R., Benna-Zayani, M., and Chehimi, M. M. (2013). Novel, ternary clay/polypyrrole/silver hybrid materials through *in situ* photopolymerization. *Colloids Surf. Physicochem. Eng. Asp.* 439, 193–199. doi: 10.1016/j.colsurfa.2013.04.005

Job, A. E., Oliveira, F. A., Alves, N., Giacometti, J. A., and Mattoso, L. H. C. (2003). Conductive composites of natural rubber and carbon black for pressure sensors. *Synth. Met.* 135–136, 99–100. doi: 10.1016/S0379-6779(02)00866-4

Knite, M., Teteris, V., Kiploka, A., and Kaupuzs, J. (2004). Polyisoprene-carbon black nanocomposites as tensile strain and pressure sensor materials. *Sens. Actuators Phys.* 110, 142–149. doi: 10.1016/j.sna.2003.08.006

Mattoso, L. H. C. (1996). Polianilinas: síntese, estrutura e propriedades. *Quím. Nova* 19, 388–399.

Mravčáková, M., Boukerma, K., Omastová, M., and Chehimi, M. M. (2006). Montmorillonite/polypyrrole nanocomposites. The effect of organic modification of clay on the chemical and electrical properties. *Mater. Sci. Eng. C* 26, 306–313. doi: 10.1016/j.msec.2005.10.044

Prudêncio, L., Camilo, F. F., and Faez, R. (2014). Ionic liquids as plasticizers in nitrile rubber/polyaniline blends. *Quím. Nova* 37, 618–623. doi: 10.5935/0100-4042.20140103

Rosa, B. D. S., Merlini, C., Livi, S., and de Oliveira Barra, G. M. (2019). Development of poly(butylene adipate-co-terephthalate) filled with montmorillonite-polypyrrole for pressure sensor applications. *Mat. Res.* 22:e20180541. doi: 10.1590/1980-5373-mr-2018-0541

Schueler, R., Petermann, J., Schulte, K., and Wentzel, H.-P. (1997). Agglomeration and electrical percolation behavior of carbon black dispersed in epoxy resin. *J. Appl. Polym. Sci.* 63, 1741–1746. doi: 10.1002/(sici)1097-4628(19970328)63:13<1741::aid-app5>3.3.co;2-s

Sethi, D., Ram, R., and Khastgir, D. (2018). Analysis of electrical and dynamic mechanical response of conductive elastomeric composites subjected to cyclic deformations and temperature. *Polym. Compos.* 39, 3912–3923. doi: 10.1002/pc.24429

Sombatsompop, N., Intawong, N. T., and Intawong, N. S. (2000). Novel sensing device for pressure measurement in molten polymer systems. *Polym. Test.* 19, 579–589. doi: 10.1016/S0142-9418(99)00028-8

Song, K. (2017). "Micro- and nano-fillers used in the rubber industry," in *Woodhead Publishing Series in Composites Science and Engineering, Progress in Rubber Nanocomposites,* eds S. Thomas and H. J. Maria (Woodhead Publishing), 41–80.

Soto-Oviedo, M. A., Araújo, O. A., Faez, R., Rezende, M. C., and De Paoli, M. A. (2006). Antistatic coating and electromagnetic shielding properties of a hybrid material based on polyaniline/organoclay nanocomposite and EPDM rubber. *Synth. Met.* 156, 1249–1255. doi: 10.1016/j.synthmet.2006.09.003

Souza, F. G. Jr., Michel, R. C., and Soares, B. G. (2005). A methodology for studying the dependence of electrical resistivity with pressure in conducting composites. *Polym. Test.* 24, 998–1004. doi: 10.1016/j.polymertesting.2005.08.001

Swart, H. C., Kumar, V., and Kalia, S. (2017). *Conducting Polymer Hybrids.* Cham: Springer International Publishing.

Thomas, S., and Maria, H. J. (eds.) (2017). *Progress in Rubber Nanocomposites, 3rd Edn*. New York, NY: Elsevier; Oxford University.

Tran, X. T., Park, S. S., Hussain, M., and Kim, H. T. (2018). Electroconductive and catalytic performance of polypyrrole/montmorillonite/silver composites synthesized through *in situ* oxidative polymerization. *J. Appl. Polym. Sci.* 135, 1–10. doi: 10.1002/app.45986

Wei, Y., Li, L., Yang, X., Pan, G., Yan, G., and Yu, X. (2010). One-step UV-induced synthesis of polypyrrole/Ag nanocomposites at the water/ionic liquid interface. *Nanoscale Res. Lett.* 5, 433–437. doi: 10.1007/s11671-009-9501-9

Conflict of Interest Statement: The authors declare that the research was conducted in the absence of any commercial or financial relationships that could be construed as a potential conflict of interest.